



ARCHIVES  
of  
FOUNDRY ENGINEERING

DOI: 10.1515/afe-2017-0139

Published quarterly as the organ of the Foundry Commission of the Polish Academy of Sciences

ISSN (2299-2944)  
Volume 17  
Issue 4/2017

109 – 114

# The Influence of Different Assist Gases on Ductile Cast Iron Cutting by CO<sub>2</sub> Laser

J. Meško, R. Nigrovič \*, A. Zrak

Department of Technological Engineering, University of Zilina  
Univerzitná 1, 010 26 Zilina, Slovakia

\*Corresponding author. E-mail address: rastislav.nigrovic@fstroj.uniza.sk

Received 15.03.2017; accepted in revised form 03.08.2017

## Abstract

This article deals with the technology and principles of the laser cutting of ductile cast iron. The properties of the CO<sub>2</sub> laser beam, input parameters of the laser cutting, assist gases, the interaction of cut material and the stability of cutting process are described. The commonly used material (nodular cast iron - share of about 25% of all castings on the market) and the method of the laser cutting of that material, including the technological parameters that influence the cutting edge, are characterized. Next, the application and use of this method in mechanical engineering practice is described, focusing on fixing and renovation of mechanical components such as removing the inflow gate from castings with the desired quality of the cut, without the further using of the chip machining technology. Experimental samples from the nodular cast iron were created by using different technological parameters of laser cutting. The heat affected zone (HAZ), its width, microstructure and roughness parameter Pt was monitored on the experimental samples (of thickness  $t = 13$  mm). The technological parameters that were varied during the experiments included the type of assist gases (N<sub>2</sub> and O<sub>2</sub>), to be more specific the ratio of gases, and the cutting speed, which ranged from 1.6 m/min to 0.32 m/min. Both parameters were changed until the desired properties were achieved.

**Keywords:** Ductile cast iron, Laser cutting, Microstructure, HAZ, Assist gas

## 1. Introduction

The principle of laser cutting of metallic materials is based on the action of a focused laser beam on the material being cut, Fig. 1. The CO<sub>2</sub> laser power density can reach values up to 10 kW<sup>3</sup>/cm<sup>2</sup>, which is a relatively high area performance. When cutting nodular cast iron in technical practice, the area impacted by a circle-shaped focused beam is of a diameter 0.1 to 0.4 mm, depending on the device construction and the thickness of the material to be cut, Fig. 2. The laser beam of the above parameters impacting the material being cut will cause its rapid heating up. The material being cut is heated in milliseconds to the melting temperature or to the evaporation temperature.

When the laser beam impacts the nodular cast iron, there occurs an interaction between that material and the laser beam. The subsequent processes that take place during the material cutting and the effect on the material properties following the focused beam impact, mainly depend on the chemical composition of the material (Table 1) being cut and on the quality of its surface which was machined by milling in our case.

In thermal cutting of metallic materials by a laser, it is always necessary first to create a hole in the processed material, from which the cutting would continue. Making the hole is based on the laser drilling principle and has slightly different characteristics of the course than that of the actual cutting. The impacting laser beam transmits the kinetic energy of the material photons, which converts into heat that melts and partially evaporates the material being heated. The surroundings of the laser beam inflammation site (in the material being cut) contain gases that get ionized at the

moment of the beam impacting the material and change to plasma. The material being cut sublimates into a gaseous state, and is blown from the material to the environment by the action of an assist gas under a relatively high pressure (in this case 80 kPa). Part of the material, which does not pass into a gaseous state, is blown in the liquid form by the flowing assist gas. The above-mentioned process causes formation of a pit in the material being cut, and the laser beam can penetrate continuously deeper, which results in depth melting of the material.

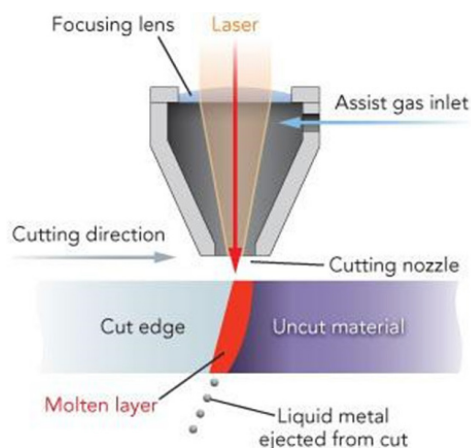


Fig. 1. Schematics of the laser cutting



Fig. 2. Application of the laser cutting on cast iron

In the present research were used two methods of laser cutting of nodular cast iron: oxidation cutting and fusion cutting.

In the oxidation process of laser cutting the material at the impact point of the laser beam gets heated to the ignition temperature and burnt in a stream of activated oxygen gas. The oxidation effect is manifested by an initial oxidation of the laser beam (reduced light reflectivity coefficient), as well as by generation of additional exothermic reaction heat from burning, which ensures an increase in the cutting speed. The cutting process is therefore the result of an exothermic reaction of the material with oxygen.

In fusion cutting, the separated material is locally melted; the resulting melt is detached from the base material by the stream of the chemically pure inert gas, which is being brought to the cutting spot, but does not take part in the cutting itself. By application of the fusion cutting only the low cutting speeds can

be reached, in comparison to other cutting processes. The maximal speed increases linearly with the laser power, and approximately linearly decreases with material's thickness.

The fusion cutting method is particularly suitable for producing a cut surface of metal materials without oxides, for instance the anti-corrosion steels, highly alloyed steels, aluminum, copper, brass and galvanized sheets.

The aim and scope of the study is laser cutting of nodular cast iron using two gases  $O_2$  (oxidative cutting) and  $N_2$  (fusion cutting), or mixtures thereof, observing the integrity of the surface and the width of the heat-affected area and the formation of adjacent slag.

## 2. Experimental investigations and discussion of results

### 2.1. Experimental material

For this particular experimental research, the cuts were executed on the laser cutting device Lasercell 1005 (TRUMPF), on samples made of cast iron with spheroidal graphite (CIwSG) with thickness  $t = 13$  mm, Fig. 3.

Table 1.

Chemical composition, wt. %

C	Si	Mn	S	P
3,18	2,82	0,09	0,012	0,011
Al	Mg	Ca	Ni	
0,07	0,049	0,0016	0,004	

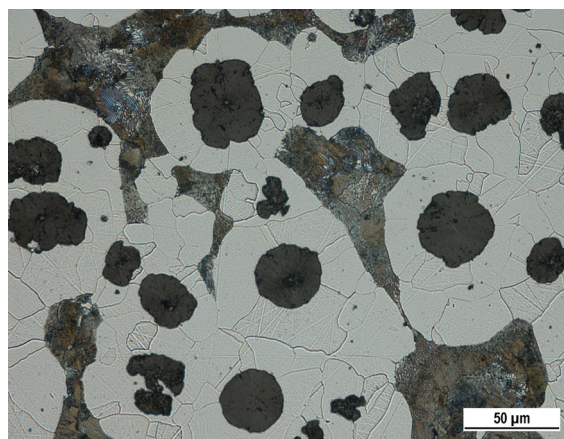


Fig. 3. Microstructure of the CIwSG – ferritic-perlitic (Fe 55) etched with 3% Nital

Metal matrix of unalloyed cast irons, after slow cooling, consists of the same structural components as steel, i.e. Ferrite and pearlite. Despite this, the knowledge of welding of steel can not be a priori applied to welding and cutting of cast iron, especially because the course of alloy crystallization does not depend only on its chemical composition but also on the rate of cooling. Increase in the transition from crystallisation to the stable

system of iron - graphite to the crystallisation into the unstable iron - cementite system. The cooling rate of the cut could be for a magnitude higher than the cooling rate of the cast iron casting.

In the cutting of nodular cast iron, the high cooling rate can also change the distribution of the flake graphite. For eutectic cast iron, with the cooling rate increase, graphite changes from the rosette graphite to the inter-dendritic. At cooling rates of 7.1 to 9 Ks<sup>-1</sup>, the needle-like cementite appears in the structure, which is most likely due to carbon enrichment of the eutectic.

When cutting nodular cast iron, they are trapped on the cutting surfaces the slag. It is a zone of partial melting. This zone often re-solidifies to form ledeburite, which negatively affects HAZ properties. Ledeburite is not excreted if the cut is cooling slowly.

The HAZ in general composed of the following four zones:

- Austenitizing zone (heated up to temperatures between eutectic and eutectoid). The structure consists of austenite decomposition products, including martensite.
- Zone of partial recrystallization (interval of eutectoid transformation). This zone is narrow; it can be difficult to detect and the grain refining occurs in it.
- Zone of graphitization and carbide spheroidization (interval of sub-eutectic temperatures, approximately above 400 up to 500 °C). Partial ferritization may occur.
- Zone of the initial structure. This is the zone heated up to temperature between 400 and 500 °C. The residual stresses decrease occurs within this zone, without changes of microstructure.

The seven combinations of parameters were used for cutting of the considered material, approximately corresponding to chemical composition and thickness of the material, for the purpose of experimental investigation of the cut integrity, from the aspect of the cut surface roughness and the HAZ microstructure.

## 2.2. Applied cutting parameters

### Experiment on sample no. 1

The sample no. 1 was cut with laser oxidation cutting using a cutting speed of 1.6 m.min<sup>-1</sup>, the nozzle used had a diameter of Ø1,4 mm. The laser power was set at 4000 W with the focal point position set 4 mm above the top edge of the nodular cast iron.

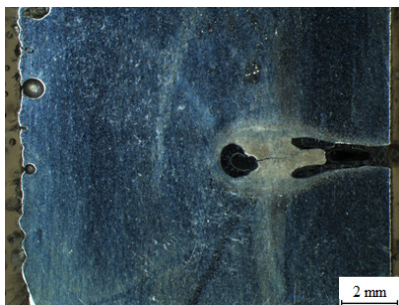


Fig. 4. Appearance of the sample no. 1 macrostructure, etched with 1% Nital

From the experimental results and photographs, one can conclude that the given parameters are not suitable for cutting the

considered material – cast iron with spheroidal graphite. The high cutting speed and inadequately chosen assist gas caused that the cut was not created at all and the laser beam penetrated only a part of the cross-section. Subsequently, in the created "keyhole" appeared a region with the dendritic structure and pronounced HAZ, Fig. 4.

### Experiment on sample no. 2

The sample no. 2 was cut with laser oxidation cutting using a cutting speed of 0,96 m.min<sup>-1</sup>, the nozzle used had a diameter of Ø1,4 mm. The laser power was set at 4000 W with the focal point position set 4 mm above the top edge of the nodular cast iron.

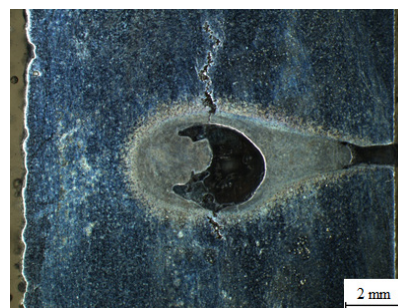


Fig. 5. Appearance of the sample no. 2 macrostructure, etched with 1% Nital

From the experimental results and photographs, one can conclude that the given parameters are not suitable for cutting the considered material. The cutting speed and inadequately chosen assisting gas caused that the cut was not created at all and the laser beam penetrated only a part of the cross-section. Again in the created "keyhole" appeared a region resembling the welded joint, with the dendritic structure and pronounced HAZ, Fig. 5. Taking into account that the laser beam has penetrated deeper into the cross section it can be predicted that the further reduction of the cutting speed would create conditions for cutting through the whole cross-section.

### Experiment on sample no. 3

The sample no. 3 was cut with laser oxidation cutting using a cutting speed of 0,64 m.min<sup>-1</sup>, the nozzle used had a diameter of Ø1,4 mm. The laser power was set at 4000 W with the focal point position set 4 mm above the top edge of the nodular cast iron.

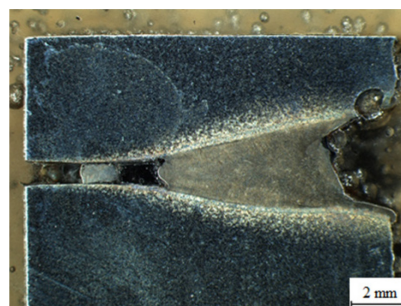


Fig. 6. Appearance of the sample no. 3 macrostructure, etched with 1% Nital

Additional decrease of the cutting speed, with keeping all other cutting parameters as for the previous sample, resulted in obtaining the cut through the whole cross-section. However, the cut again was not coherent, because the molten metal once again entered in between the cut surfaces and solid joined the cut material, Fig. 6. From those results, one can conclude that the given parameters were not suitable for cutting of the tested material, from the aspect of the completeness of the cut, the HAZ width and the width of the cutting gap.

#### Experiment on sample no. 4

The sample no. 4 was cut with laser oxidation cutting using a cutting speed of  $0,32 \text{ m}\cdot\text{min}^{-1}$ , the nozzle used had a diameter of  $\varnothing 1,4 \text{ mm}$ . The laser power was set at 4000 W with the focal point position set 4 mm above the top edge of the nodular cast iron.

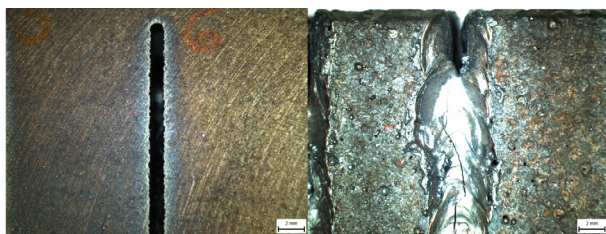


Fig. 7. The resulting cut obtained with the given cutting parameters:  
(left – appearance of the cut surface perpendicular to the input laser beam,  
right – appearance of the cut surface at the laser beam exit)

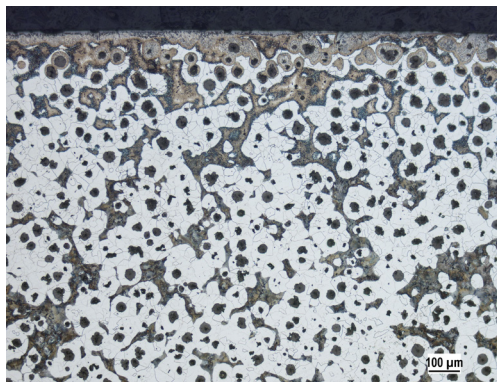


Fig. 8. Microstructure of the sample no. 4, etched with 3% Nital

From experimental results and photographs in Figs. 7 and 8, one can conclude that cutting with the assist gas  $\text{O}_2$  is not suitable for the tested material – cast iron with spheroidal graphite. Inadequate assist gas caused that the incomplete cut was obtained and that the laser beam penetrated only partially through the cross-section, or the cut was re-joined by the melted material. In the created "key-hole" appeared a region resembling the welded joint with the dendritic structure and the pronounced HAZ. On sample # 4 also appeared substantial hot crack, which caused the fracture of the cut. From the microstructure recordings, one can state that the oxidation cutting with use of the  $\text{O}_2$  is not suitable from the aspect of the material's structure, as well. Due to the high temperatures and  $\text{O}_2$  assist gas, the extreme decarburizing of the

material by chemical reaction has occurred, subsequently, the weakened graphite was removed from the structure during the preparation of samples.

The primary form of the cutting area was immeasurable.

#### Experiment on sample no. 5

The sample no. 5 was cut with laser fusion cutting with assist gasses  $20\% \text{N}_2 + 80\% \text{O}_2$ , using a cutting speed of  $1 \text{ m}\cdot\text{min}^{-1}$ , the nozzle used had a diameter of  $\varnothing 1,4 \text{ mm}$ . The laser power was set at 3200 W with the focal point position set 4 mm above the top edge of the nodular cast iron.

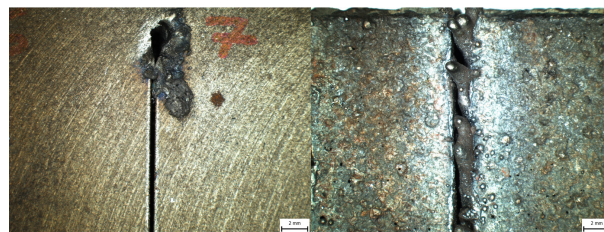


Fig. 9. The resulting cut obtained with the given cutting parameters:  
(left – appearance of the cut surface perpendicular to the input laser beam,  
right – appearance of the cut surface at the laser beam exit)

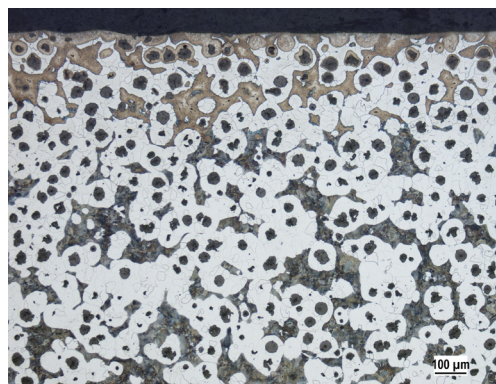


Fig. 10. Microstructure of sample no. 5, etched with 3% Nital

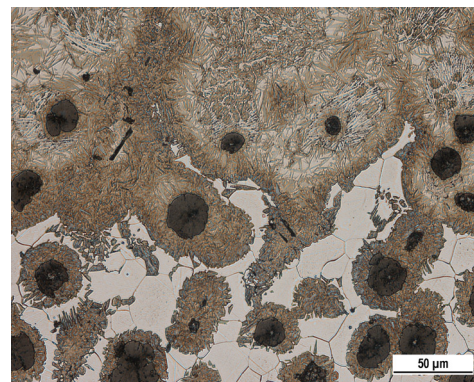


Fig. 11. Detailed microstructure of sample no. 5 with visible martensitic packing of graphite, etched with 3% Nital

From experimental results and photographs in Figs. 9, 10 and 11, one can see that cutting with the assist gas  $20\%N_2+80\%O_2$  created the complete cut through the whole cross-section of the sample, from what one can conclude that the type of the assist gas and its ratio have essential influence on the quality of the cut. On the edge of the cut was an apparent HAZ, consisting of martensitic and bainite structure, which is significantly harder than the base material. The graphite particles in the HAZ were chemically and chemically-mechanically removed due to high temperatures (decarburizing). The primary form of cut surface was  $P_t = 0.1238$  mm.

#### Experiment on sample no. 6

The sample no. 5 was cut with laser fusion cutting with assist gasses  $40\%N_2+60\%O_2$ , using a cutting speed of  $1 \text{ m}\cdot\text{min}^{-1}$ , the nozzle used had a diameter of  $\varnothing 1,4$  mm. The laser power was set at **3200 W** with the focal point position set **4 mm** above the top edge of the nodular cast iron.

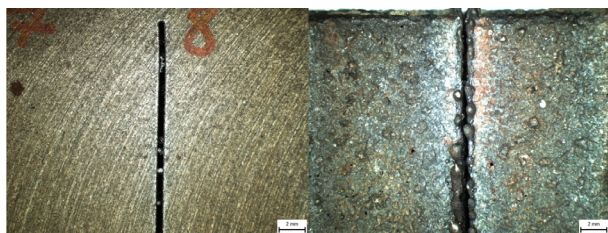


Fig. 12. The resulting cut obtained with the given cutting parameters:  
(left – appearance of the cut surface perpendicular to the input laser beam,  
right – appearance of the cut surface at the laser beam exit)

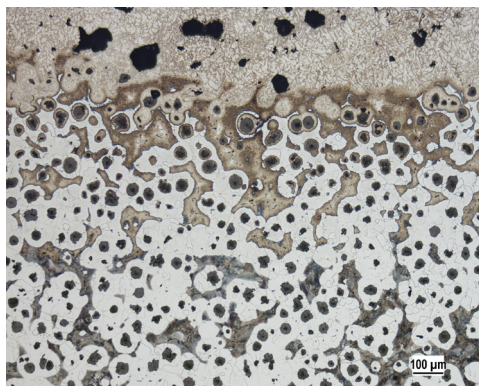


Fig. 13. Microstructure of the sample no. 6, etched with 3% Nital

From experimental results and photographs in Figs. 12 and 13, one can see that cutting with the assist gas  $40\%N_2+60\%O_2$  created the complete cut through the whole cross-section of the sample. Slag that settled at the bottom side of the cut had a different structure than the rest of the cutting edge, which had the bainite structure. At the edges of the cut was an evident HAZ, consisting of martensitic and bainite structure, which is significantly harder than the base material. The graphite particles in the HAZ were chemically and chemically-mechanically

removed due to high temperatures (decarburizing). The primary form of cut surface was  $P_t = 0.6383$  mm.

#### Experiment on sample no. 7

The sample no. 7 was cut with laser fusion cutting with assist gasses  $30\%N_2+70\%O_2$ , using a cutting speed of  $1 \text{ m}\cdot\text{min}^{-1}$ , the nozzle used had a diameter of  $\varnothing 1,4$  mm. The laser power was set at **3200 W** with the focal point position set **4 mm** above the top edge of the nodular cast iron.

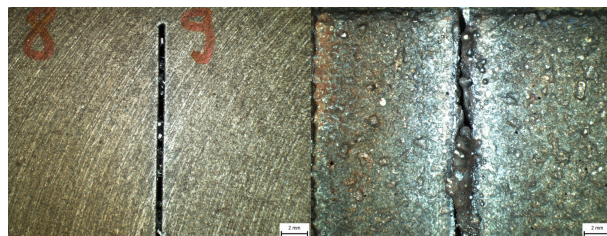


Fig. 14. The resulting cut obtained with the given cutting parameters:  
(left – appearance of the cut surface perpendicular to the input laser beam,  
right – appearance of the cut surface at the laser beam exit)

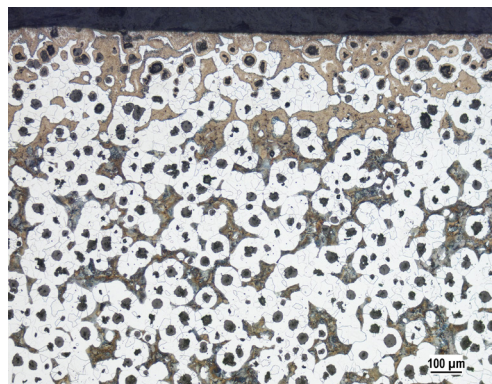


Fig. 15. Microstructure of the sample no. 7, etched with 3% Nital

From experimental results and photographs in Figs. 14 and 15, one can see that cutting with the assist gas  $30\%N_2+70\%O_2$  created the complete cut through the whole cross-section of the sample. At the edges of the cut was an evident HAZ, consisting of ferritic, perlitic and bainite structure, which is significantly harder than the base material. The graphite particles in the HAZ were chemically and chemically-mechanically removed due to high temperatures (decarburizing). The primary form of cut surface was  $P_t = 0.1161$  mm.

### 3. Conclusions

From the results of experiments, conducted within this research, one can state that the laser cutting of the cast iron with spheroidal graphite, of the presented chemical composition and thickness  $t = 13$  mm, is appropriate to apply for the single casting and for reparation and renovation of the castings' walls, in the

case that they were damaged. The  $t = 13$  mm thickness was deliberately chosen as the simulation thickness for the in-flow separation and the delivery system risers' simple castings.

In the presented paper there were compared different technological parameters of the laser cutting of the experimental cast iron. Closer evaluations were done for each experiment separately. All experiments demonstrated the transformed grains in the HAZ, where each of the reshaped structures had higher hardness than the base material (ferritic-perlitic Fe55 structure).

## Acknowledgements

The research presented in this paper was partially financially supported through realization of project VEGA no. 1/0186/09-(V-13-013-00) - responsible investigator: Jozef Meško

## References

- [1] Silvfast, W.T. (2004). *Laser Fundamentals*, Cambridge University Press, 666p. ISBN 0-521-83345-0.
- [2] Caristan, L.C. (2004). *Laser cutting guide for manufacturing*. Dearborn, Michigan, USA: Society of Manufacturing Engineers, 452p. ISBN 0-87263-686-0.
- [3] Konar, R., Patek, M. & Zrak, A. (2015). Ultrasonic testing of non-ferrous materials in the foundry industry. *Manufacturing Technology: Journal for Science, Research and Production*. 15(4), 557-562. ISSN 1213-2489.
- [4] Zrak, A., Konar, R. & Jankejech, P. (2015). Influence of chemical composition in steel on laser cutting stability. *Manufacturing Technology: Journal for Science, Research and Production*. 15(4), 748-752. ISSN 1213-2489.
- [5] Konar, R., Mician, M. & Hlavaty, I. (2014). Defect detection in pipelines during operation using Magnetic Flux Leakage and Phased Array ultrasonic method. *Manufacturing technology*, 14(3), 337-341. J.E. Purkyne University, Ústínad Labem. ISSN 1213-2489.
- [6] Mesko, J., Zrak, A., Mulczyk, K. & Tofil, S. (2014). Microstructure analysis of welded joints after laser welding. *Manufacturing technology*, 14(3), 355-359. 341. J.E. Purkyne University, Ústínad Labem. ISSN 1213-2489.
- [7] Patek, M., Konar, R., Sladek, A. & Radek, N. (2014). Non-destructive testing of split sleeve welds by the ultrasonic TOFD method. *Manufacturing technology*, 14(3), 355-359. J.E. Purkyne University, Ústínad Labem. ISSN 1213-2489.
- [8] Lago, J., Guagliano, M., Novy, F. & Bokuvka, O. (2016). Influence of laser shock peening surface treatment on fatigue endurance of welded joints from S355 structural steel. *Manufacturing technology: journal for science, research and production*. 16(1), 154-159. ISSN 1213-2489.
- [9] Radek, N., Bronček, J., Fabian, P., Sladek, A., Radziszewski, L. & Paraska, O. (2016). Laser welding of mild steel. *Technológ, Roč.* 8(3), 23-28. ISSN 1337-8996.
- [10] Zapoměl, J., Dekýš, V., Ferfecki, P., Sapietová, A., Sága, M. & Žmindák, M. (2015). Identification of Material Damping of a Carbon Composite Bar and Study of Its Effect on Attenuation of Its Transient Lateral Vibrations. *International Journal of Applied Mechanics*. 7(6), 1550081 (18 pages). DOI: 10.1142/S1758825115500817.
- [11] Danielewski, H., Banak, R. & Domagala, A. (2013) The Experimental Analysis of Striation Pattern Created During Laser Cutting. In: *Transcom*, Žilina, Slovakia.
- [12] Skocovsky, P., Bokuvka, O., Konecna, R., Tillova, E. (2006) *Material training for engineering departments*. EDIS vydavateľstvo ŽU, 349s. ISBN 80-8070-593-3